COMMUNICATIONS CHEMISTRY

ARTICLE

https://doi.org/10.1038/s42004-018-0101-4 OPEN

Direct manipulation of liquid ordered lipid membrane domains using optical traps

Mark S. Friddin[1,2], Guido Bolognesi[3], Ali Salehi-Reyhani[4,5], Oscar Ces[1,2,4] & Yuval Elani[1,2,4]

Multicomponent lipid bilayers can give rise to coexisting liquid domains that are thought to influence a host of cellular activities. There currently exists no method to directly manipulate such domains, hampering our understanding of their significance. Here we report a system that allows individual liquid ordered domains that exist in a liquid disordered matrix to be directly manipulated using optical tweezers. This allows us to drag domains across the membrane surface of giant vesicles that are adhered to a glass surface, enabling domain location to be defined with spatiotemporal control. We can also use the laser to select individual vesicles in a population to undergo mixing/demixing by locally heating the membrane through the miscibility transition, demonstrating a further layer of control. This technology has potential as a tool to shed light on domain biophysics, on their role in biology, and in sculpting membrane assemblies with user-defined membrane patterning.

[1] Department of Chemistry, Molecular Sciences Research Hub, Imperial College London, Wood Lane, White City, London W12 0BZ, UK. [2] Institute of Chemical Biology, Molecular Sciences Research Hub, Imperial College London, Wood Lane, White City, London W12 0BZ, UK. [3] Department of Chemical Engineering, Loughborough University, Loughborough LE11 3TU, UK. [4] fabriCELL, Imperial College London, Wood Lane, White City, London W12 0BZ, UK. [5] Department of Chemistry, King's College London, Britannia House, 7 Trinity Street, London SE1 1DB, UK. Correspondence and requests for materials should be addressed to O.C. (email: o.ces@imperial.ac.uk) or to Y.E. (email: y.elani@imperial.ac.uk)

Optical trapping employs a tightly focused laser beam to trap and manipulate particles ranging from tens of nanometres to tens of micrometres in diameter in 3D space[1]. The technique, also referred to as optical tweezing, enables forces in the range of a few hundred pN to be generated with a resolution down to 50 fN in contemporary systems[2,3]. The combination of these features results in a potent and reliable approach for the contactless manipulation of particles with high spatial and temporal precision across a range of length scales; properties that are ideal for probing biological systems[4]. To this end, optical traps have been used to manipulate individual cells, viruses and organelles[1,5–7], to extract and sample materials from plasma membranes[8], and to elucidate the biophysics of protein folding[9], molecular motors[10], and ribosome translation one codon at a time[11]. Further, optical traps have also been used to study the surface tension, elasticity and bending modulus of soft matter systems such as biological membranes by generating long tether-like nanotubes[12]. Optical traps have more recently been used to construct 2D and 3D model membrane architectures, including networks of droplet interface bilayers[13,14] and giant unilamellar vesicles (GUVs)[15], which can be positioned into contact and fused together to deliver material payloads via lipid-conjugated gold nanoparticles[15,16]. This new frontier in the use of optical traps is leading the technique to be considered as a powerful tool for bottom-up synthetic biologists, enabling increasingly complex cell and tissue-mimetic architectures to be engineered on-demand. These studies, however, have all involved gross manipulation of entire membrane structures in space.

Despite this progress, to date, there have been no reports of direct optical trapping of laterally segregated domains within lipid bilayers, i.e., where the membrane itself acts as the 2D fabric in which embedded structures are manipulated. In this case, membrane domains are defined as coexisting phase separated regions in lipid membranes[17]. Achieving this will pave the way for optical traps to be used as tools to probe domain biophysics and have implications for the design and construction of membrane microsystems with user-defined membrane patterning.

Lipid domains, which are thought to be linked to cell membrane rafts[18,19], arise due to a fundamental property of certain lipids to transition between a gel phase (L_β) and a liquid phase (L_α) at a defined melting temperature (T_m). These phases can coexist at certain temperatures in dual component bilayers made up of high and low T_m lipids. When cholesterol is added, phase-separated liquid disordered (L_d) and liquid ordered (L_o) domains can be formed. The system can be reverted back and forth from a phase separated to a mixed state by performing heating cycles past the characteristic miscibility temperature (T_{misc})[20].

There is mounting evidence to suggest that this lateral organisation plays a key role in biological membranes, with lipid rafts thought to be involved in a range of cellular activity from signalling and trafficking, to providing a mechanical support for the anchoring of membrane proteins[18,19,21–24]. Yet due to the lack of experimental data obtained in-vivo, the biological significance of lipid domains remains a contentious topic.

There have been extensive efforts at using model systems to study membrane domains, using systems such as supported lipid bilayers[25], planar lipid membranes[26,27], GUVs[28,29], and droplet-hydrogel bilayers[30]. The advantage of using model systems in this context is that the size, composition, degree of compartmentalisation, and level of asymmetry of the assembled membrane can be carefully controlled by the investigator, especially when microfluidic methods are employed[31]. This has led to advances in our understanding of fundamental membrane behaviour, and of the properties that govern their cellular functions. However, methods to manipulate individual domains formed both in native and model bilayers do not yet exist, which partly explains why their biological significance is still poorly understood.

Indirect domain motion arising from thermal gradients[32,33], electric fields[34], and fluid flows[35,36] have been elegantly demonstrated, but these methods lack the spatiotemporal control afforded by optical traps. Manipulation of non-phospholipid domains on a langmuir monolayer (water/air interface), using optical traps via silica beads as 'handles' localised in the phase coexistence region[37–39], and via director structures and defects in liquid crystals[40] has also been demonstrated.

However, the ability to directly manipulate biologically relevant lipid domains within a bilayer system has yet to be realised. Manipulating membrane subcompartments could be key in unravelling the biological significance of lipid domains, and could have a host of potential applications from mediating the spatial exchange of materials across lipid bilayers, to studying mobility and affinity of membrane components to lipid rafts.

Here, we demonstrate the use of light to directly trap and manipulate individual L_o domains embedded within an L_d matrix of GUVs that have been adsorbed on a glass substrate. We showcase the ability to selectively drag individual lipid domains across a membrane at will and show that the trapping laser can also be used to locally and reversibly heat the bilayer surface past T_{misc} to induce domain mixing/demixing on-demand.

Results

Optical trapping of domains. Ternary GUVs comprised of 1,2-dioleoyl-sn-glycero-3-phosphocholine (DOPC), 1,2-dipalmitoyl-sn-glycero-3-phosphocholine (DPPC) and cholesterol (2:1:1 mole ratios) were electroformed in 0.4 M sucrose in deionised (DI) water. GUVs were then added to a microscope well, and diluted 1:9 with 0.4 M glucose. Domain visualisation was achieved using fluorescence microscopy by incorporating 1 mol% Rhodamine-PE into the membrane, which partitions into the DOPC-rich disordered phases. Consistent with previous findings, we found that our GUVs were phase separated at room temperature (21 °C) with an L_o phase enriched with cholesterol and DPPC (T_m = 41 °C) and an L_d phase enriched in DOPC ($T_m = -17$ °C). A single-beam optical trap was coupled to a 60x 1.4 N.A. oil immersion microscope objective using custom optics and a Ytterbium fibre laser source (20 W at 1070 nm) as we have described previously[13]. In our setup, the position of the trap stays fixed while the motorised microscope stage is moved in two dimensions. Imaging was achieved using a CCD camera (ORCA-ER Hamamatsu) in combination with homemade LabVIEW software.

Applying the laser to a free-floating GUV had the effect of simply trapping the GUV at the laser focal point, meaning focusing and trapping individual domains was not possible. To circumvent this, we designed a system that allowed GUVs to be bound to a glass substrate. Replacing glucose with NaCl in the external solution (0.2 M) led to adhesive interactions between the glass and the membrane. This led to two observed situations[41,42] (i) immobilisation, adsorption, and flatting out of the GUV on the substrate and (ii) collapse of the GUV to yield a supported lipid bilayer (SLB). The GUVs were occasionally seen to transition from the first to the second geometries, as depicted in Fig. 1a and Supplementary Movie 1. Above 0.5 mM NaCl, only the second scenario was observed. Domains in SLBs have previously been found to be affected by the underlying glass, rendering them immobile[43,44]. Although they mix above T_{misc}, they do not macroscopically demix upon cooling due to the reduced lipid mobility[43]. This behaviour was seen in our system as well, and trapping of such domains was not possible with optical forces used.

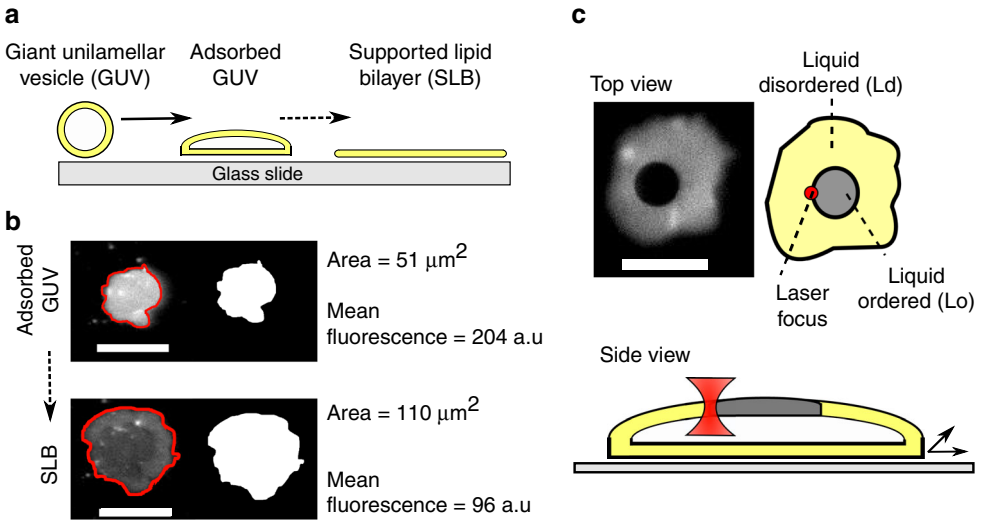

Fig. 1 Experimental setup (**a**) Schematic of transitions observed in the presence of 0.2 M NaCl. Adsorbed GUVs did not always transition to SLBs, and it is on these structures that domains could be manipulated. **b** Fluorescence images of adsorbed GUVs transitioning into SLBs. As expected, the area enclosed by fluorescence perimeter (red) increased, and the mean fluorescence intensity per unit area decreased upon SLB deposition. **c** Fluorescence image and schematic of Lo/Ld domain on an adsorbed GUV, with the laser (red) trapping the domain interface. Domains were manipulated at 0.23 W (at trap) laser powers. All scale bars = 10 μm

When GUVs adsorbed and did not collapse on the glass substrate however, domains remained mobile. Adsorbed GUVs adopt a flattened structure[41,42] with the upper portion of the membrane unaffected by the underlying substrate. This architecture is supported by the observation that on occasions where the GUV transitioned between an adsorbed GUV and collapsed SLB, fluorescence intensity per area decreased and the area of the fluorescence patch increased, as shown in Fig. 1b. This observation suggests that the flattened GUV contains fluorescence intensity contributions from two bilayers and, hence, the objective depth of field (ca. 0.5 μm) is of the same order of the flattened GUV thickness.

The lack of interaction between the domain and the glass substrate allowed optical manipulation. Upon positioning the optical trap at the interface of the two phases and turning the power up to 0.23 W (at the trap), we found that we could trap and dynamically manipulate the position of the L_o phase in 2D by moving the microscope stage (Fig. 2a; see Supplementary Movies 2 and 3).

Trapping was observed reproducibly provided GUVs were adhered to the surface (i.e., not free floating) and did not rupture to yield SLB. A minimum of 15 GUVs for each composition tested was explored. Domains were dragged from the edge, not from the centre, indicating that the interface itself was being trapped, and slight deformations of the domains away from a fully spherical geometry were seen upon movement due to drag forces (Supplementary Movie 4). Domains could be manipulated to reside in different regions of the GUV (Fig. 2). It is noted that at equilibrium, as well as during manipulation, the L_o/L_d interface remained always located near the laser beam waist. This observation suggests that domain trapping and manipulation are the result of optical gradient forces, originating from the difference in both membrane refractive index and thickness between the L_o and L_d phases[45,46], as opposed to laser-induced thermal effects. Indeed, it is known that membrane domains have different thicknesses, with more ordered domains tending to be thicker[47–49]. The effect of the height mismatch on trapping is a consequence of the fact that both phases have a different refractive index to the surrounding medium. Furthermore, had

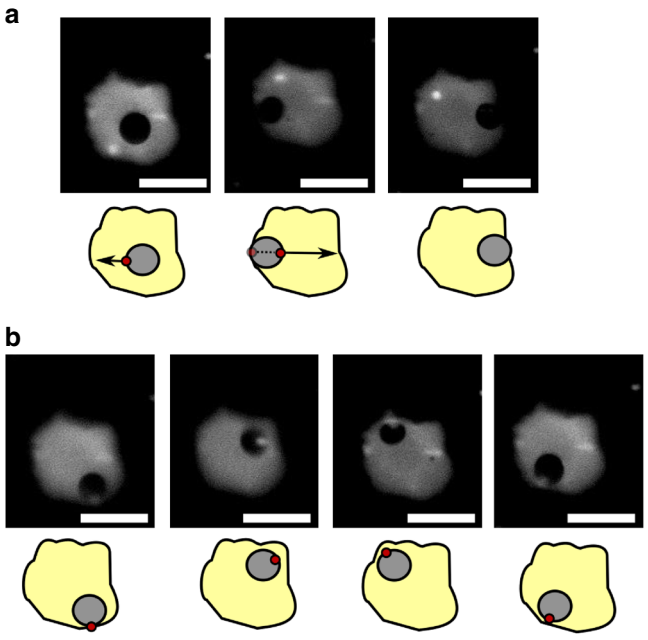

Fig. 2 Optical manipulation of membrane domains (**a**) Fluorescence images showing side-to-side movement of a liquid ordered domain on an adsorbed GUV. Schematic showing location of laser (red) and direction of movement (arrow) is shown below. Domains are dragged by the optical traps at the interface of the two phases. **b** Dragging the domain by the interface leads to a slight deformation away from a spherical geometry due to drag forces. All scale bars = 10 μm

the domain motion been driven by a thermophoretic effect, at equilibrium the laser beam would have been located at the centre of the circular L_o domain for symmetry reasons. It was observed that the domain interface could not be trapped when the laser beam was positioned a short distance away (~μm). This is consistent with the rapid exponential decay of the optical gradient

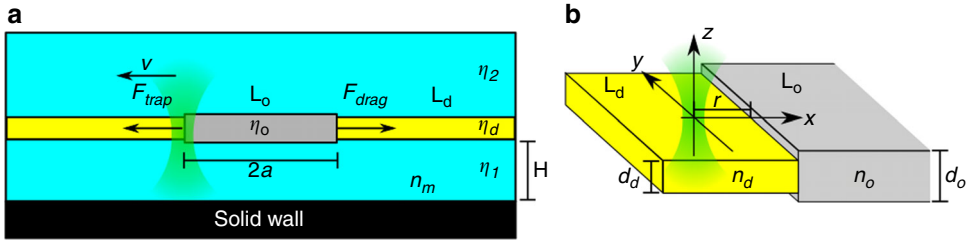

Fig. 3 Estimation of force balance (**a**) A cylindrical lipid domain dragged at constant speed by an optical trap (**b**) Simplified model of the trapped object for optical force calculation, consisting of two semi-infinite domains of different thickness and refractive index

force with the distance r between the trap and the domain interface, discussed in the next section. All these observations support our interpretation of optical trapping as the driving mechanism for lipid domain manipulation. We also noted that the domain could not be manipulated in the direction parallel to the optical axis of the laser beam or outside of the GUV perimeter.

We also tried trapping gel domains in a liquid matrix in GUVs composed of DOPC/DPPC 1:1. The phase separated GUVs consisted of an interlinked mesh of gel domains, exhibiting a percolation pattern. We were not able to determine successful trapping due to their small size and difficulty in resolving their spatiotemporal positioning on the epi-fluorescent microscope.

Force balance on optically-trapped moving domain. When a lipid domain is pulled by an optical trap (Fig. 3a), the component F_{trap} of the optical trapping force, parallel to the lipid bilayer, is balanced by the viscous drag F_{drag}. To verify this physical description, we derive a quantitative estimate of the photonic and hydrodynamic forces under our experimental conditions and demonstrate that they are of the same magnitude. A coordinate reference system with the origin in the trap centre, as shown in Fig. 3b, is introduced. Since the beam radius ω is much smaller than the domain radius a, both ordered and disordered phases are modelled as two semi-infinite membranes with refractive indices n_o and n_d, viscosities η_o and η_d, and thicknesses d_o and d_d, respectively. The membranes are surrounded by an aqueous subphase and superphase of viscosity η_1 and η_2, respectively. The domain interface is perpendicular to the x-axis and the distance between the trap centre and the interface is denoted as r. By using the approach of Tlusty et al.[50], an approximated expression of the optical trapping force F_{trap} exerted by the laser on the trapped domain can be derived as

$$F_{trap} = -\frac{\partial W}{\partial r} \tag{1}$$

where

$$W = \frac{\varepsilon_0}{2}\int_{V_{obj}} \left(n_m^2 - n_{obj}^2\right)\left|\vec{E}\right|^2 dV \tag{2}$$

is the interaction energy between the laser trap and the trapped object (i.e., the L_o and L_d phase membranes) with ε_0 the vacuum permittivity, n_m the refractive index of the surrounding aqueous phase, n_{obj} and V_{obj} the refractive index and volume of the trapped object, respectively. $\vec{E}$ is the electric field of the trapping beam, which is difficult to evaluate as it includes both the incident beam as well as the scattered field. However, due to the nanometre thickness of the membrane, the unperturbed incident field $\vec{E}_0$ may be considered. For sake of simplicity, the electric field $\vec{E}$ can be described by an approximated axially-symmetric Gaussian beam[51]

$$\left|\vec{E}\right|^2 = \frac{4P}{c\, n_m\, \pi\, \varepsilon_0\, \omega^2}\exp\left(-\frac{2\rho^2}{\omega^2}\right)\exp\left(-\frac{2z^2}{\omega^2\xi^2}\right) \tag{3}$$

with P the laser power, c the speed of light, $\rho = \sqrt{x^2+y^2}$ the radial distance from the beam axis, z the axial distance from the trap centre, ω the beam radius and ξ the beam eccentricity[50]. In principle, this simplified description of the electric field is not valid for our experimental conditions since the vector character of the electromagnetic field cannot be neglected for a highly focused beam[52]. Nevertheless, previous studies[40,50] have shown that Eq. (2) can be adopted to gain a qualitative insight on the trapping force exerted by a tightly focused laser beam. By performing the integration in Eq. (2) with $n_{\mathrm{obj}} = n_d$ for $x < r$ and $n_{obj} = n_o$ for $x \geq r$, it follows

$$W = \sqrt{\frac{\pi}{8}}\frac{P n_m\, \omega\, \xi}{c}\left[\left(1-\frac{n_d^2}{n_m^2}\right)\left(1+\mathrm{erf}\left(\frac{r\sqrt{2}}{\omega}\right)\right)\mathrm{erf}\left(\frac{d_d}{\sqrt{2}\,\omega\,\xi}\right) + \right. \\ \left. + \left(1-\frac{n_o^2}{n_m^2}\right)\left(1-\mathrm{erf}\left(\frac{r\sqrt{2}}{\omega}\right)\right)\mathrm{erf}\left(\frac{d_o}{\sqrt{2}\,\omega\,\xi}\right)\right] \tag{4}$$

and, hence according to Eq. (1)

$$F_{trap} = \frac{\partial W}{\partial r} = f\frac{P n_m\, \xi}{c}\exp\left(-\frac{2r^2}{\omega^2}\right) \tag{5}$$

with the pre-factor f given by

$$f = \left(\frac{n_d^2}{n_m^2}-1\right)\mathrm{erf}\left(\frac{d_d}{\sqrt{2}\omega\xi}\right) - \left(\frac{n_o^2}{n_m^2}-1\right)\mathrm{erf}\left(\frac{d_o}{\sqrt{2}\omega\xi}\right) \tag{6}$$

It can be seen that the peak value of the trapping force is achieved when the trap centre is located at the domain interface (i.e., $r = 0$). Furthermore, the pre-factor f shows that the trapping effect arises from the difference in both membrane refractive index and thickness between the L_o and L_d phases. Interestingly, the optical force may vanish if the difference in refractive index between the lipid phases (e.g., $\Delta n = n_o - n_d > 0$) is compensated by an opposite mismatch between the phase thicknesses (i.e., $\Delta d = d_o - d_d < 0$) so that $f \simeq 0$. Under the examined experimental conditions, we have $\omega = 300$ nm, $\xi = 3$, $P = 0.23$ W and $n_m = 1.33$. To a first approximation, we can assume that the L_o and L_d phases have refractive indices of the corresponding pure DPPC and DOPC lipid phases[53], namely $n_o = 1.4088$ and $n_d = 1.4165$. Finally, by assuming thicknesses of $d_d = 4.36$ nm and $d_o = 6.05$ nm for the disordered and ordered phases[54], respectively, Eq. (5) gives a peak value of $|F_{\mathrm{trap}}| \simeq 0.4$ pN.

Stone et al.[55] determined the drag force exerted on a solid lipid domain of radius a bound in an infinite membrane of thickness h and viscosity η sitting between a semi-infinite inviscid fluid (superphase) and a viscous fluid (subphase) of finite depth H and viscosity η'. According to these calculations, the drag force can be expressed as

$$F_{drag}^{w} = 4\pi\eta' a\, U f(\delta, \Lambda_w) \tag{7}$$

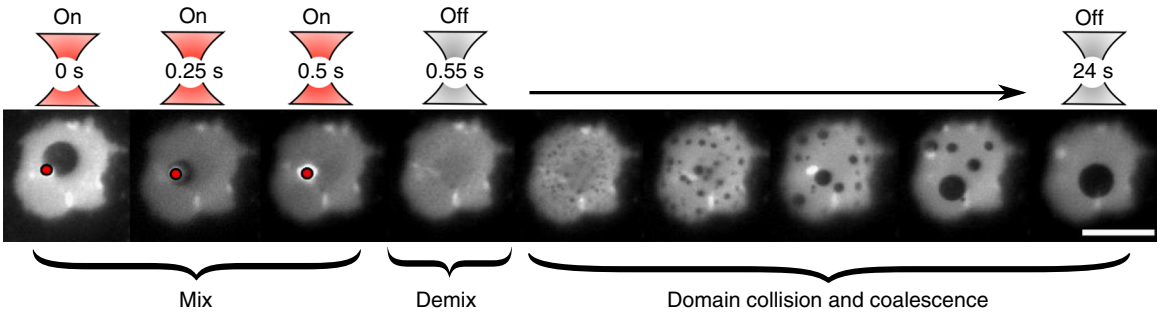

Fig. 4 Domain mixing using laser-induced heating fluorescence images showing complete domain mixing within 0.5 s of exposure to a laser. Within 0.05 s of turning the laser off, demixing is observed. Domain collision and coalescence was then observed until a single domain remains after 24 s. Scale bar = 10 μm

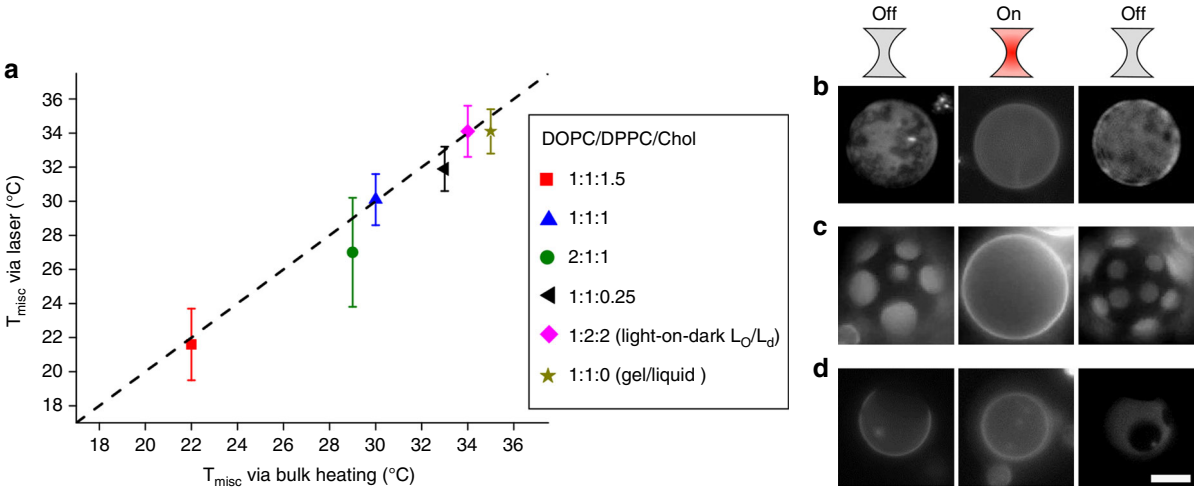

Fig. 5 T_{misc} of different GUV compositions reached via laser-induced heating (**a**) Graph of T_{misc} reached by applying lasers of different powers vs literature T_{misc} values obtained through bulk heating. These values correspond to each another, represented by the dotted line. Error bars = SD; $n = 10$. **b**–**d** Fluorescent images of domains before, during, and after laser applied (demixed, mixed, demixed respectively). Compositions are (**b**) DOPC/DPPC 1:1, gel/liquid (**c**) DOPC/DPPC/Chol, 1:2:2, Lo/Ld domains (light-on-dark) and (**d**) DPhPC/DPPC/Chol, 1:1:2, Lo/Ld domains (saturated phospholipids). Scale bar = 5 μm

where U is the domain velocity and $f(\delta, \Lambda_w)$ a known function of $\delta = H/a$ and $\Lambda_w = a\eta'/h\eta$, which can be computed numerically[55]. To calculate Λ_w, the viscosity η of the DOPC-rich L_d phase membrane can be approximated with the viscosity of pure DOPC (0.160 Pa s at 20 °C)[56]. According to the numerical calculations by Stone et al.[55], for a domain of radius $a = 2.5\,\mu$m moving at $U \simeq 2.5$ μm/s, by taking $h = d_d = 4.57$ nm, $\eta' = \eta_1 =$ 1.5 mPas (i.e., viscosity of 0.4 M sucrose solution at 20 °C)[57] and assuming $\delta \simeq 0.3$ it results $\Lambda_w \simeq 5.3$ and $f(0.3, 5.3) \simeq 2.7$. Hence, Eq. (7) gives $F^w_{drag} \simeq 0.3$ pN. It is recognised that some of the assumptions used to develop the theoretical model leading to Eq. (7) are not met under our experimental conditions, nevertheless it can be seen that the differences between the adopted theoretical description and our experimental system do not affect the magnitude of our drag force calculation. In the theoretical model[55], a no-slip boundary condition between the domain and the sub-/super-phases is adopted to describe the dynamics of a solid domain. Conversely, for a liquid domain in a lipid matrix with similar viscosities, as in our experiments, an intermediate behaviour between no-slip and perfect slip (i.e., zero tangential stress) is expected. However, it is has been shown that the drag depends only weakly on the choice of boundary condition at the domain surfaces[58,59] and, hence, Eq. (7) can provide a good estimate of the drag for liquid domain as well. In our flattened GUVs, the trapped L_o domains are not small compared to the L_d membrane and finite-size effects are expected to generate a drag larger than F^w_{drag}, but still of the same magnitude[32]. Finally, in our experiments the superphase (sodium chloride solution) is not inviscid, as described in the model, but has a similar viscosity to the one of the subphase (sucrose solution). The additional drag F^∞_{drag} caused by the semi-infinite viscous superphase can be estimated by replacing $\eta' = \eta_2 = 1$ mPas and $\delta \to \infty$ in Eq. (7), from which $F^\infty_{drag} = 0.1$ pN, which has the same magnitude of F^w_{drag}. Hence, to a first approximation the total drag exerted on a liquid domain in a flattened GUV can be estimated as $F_{drag} = F^w_{drag} + F^\infty_{drag} \simeq 0.4$ pN, which, as expected, it is comparable to the optical trapping force F_{trap}. This drag force estimate corresponds to a drag coefficient $\lambda = F_{drag}/U \simeq 1.6 \times 10^{-7}$ N s/m. Our theoretical predictions were validated by tracking the Brownian motion of a free (i.e., not trapped) L_o domain on a L_d membrane. By analysing the domain's mean square displacement, the domain's diffusivity D was calculated and, hence, the corresponding drag coefficient was derived through the Einstein relation $\lambda = k_bT/D$, where k_b is the Boltzmann constant and T the temperature. For a domain of 2.35 μm in radius, it was measured a drag coefficient of 1.7×10^{-7} N s/m, which is of the same order of the one predicted by the model (Supplementary Fig. 1).

Laser-induced domain mixing. In addition to manipulating the L_o phase, we could also locally heat the GUV past the T_{misc} (ca. 29 °C)[17] and induce mixing by increasing the power of the laser source above 0.47 W at the trap (Fig. 4; Supplementary Movie 5). This leads to a temperature increase of approximately 7 °C at the laser focus (Supplementary Table 1). Domains fully mixed within 0.5 s of applying the laser, and reappeared within 0.05 s after the laser was turned off. This rapid dynamics is due to the short timescale $\tau = l^2/\alpha \simeq 0.2$–20 ms for heat dissipation in water solution (thermal diffusivity $\alpha = 0.14 \times 10^{-6}\,m^2\,s^{-1}$) at length scales $l = 5$–50 μm. Smaller circular domains were mobile, and gradually coalesced with one another until a single Lo/Ld domain remained after 24 s. The optical forces and laser powers that could be applied to the domains therefore has to be below those in which local heating leads to mixing.

To demonstrate the generality of our approach we were able to achieve laser-induced phase transitions in GUVs composed of six different DOPC/DPPC/Chol lipid molar fractions, and hence different T_{misc}. GUVs showing gel/liquid coexistence, as well as L_o/L_d coexistence were examined. We focussed the optical trapping laser at the GUV centre and increased the laser power at 20 mW (at trap) increments and determined at what power a threshold was reached and miscibility of the coexisting phases was observed to give a fully mixed system. We then translated these laser power values to a temperature increase through a calibration curve (Supplementary Table 1). Our results map on to the T_{misc} values obtained from literature (Fig. 5)[17], which validates our laser-induced heating approach. These results also indicate that lipid thermal absorption effects are not significant in this context. Control experiments with GUVs containing fully saturated DPhPC instead of unsaturated DOPC confirmed that these phase separation transitions were not due to photo-oxidation effects (Fig. 5d; Supplementary Note 1). Critically, this approach allows us to select individual vesicles in a population to undergo mixing, adding an element of spatiotemporal control compared to bulk heating approaches.

We found that at laser powers below the threshold where T_{misc} is reached, no change in the phase state of the domain was seen, regardless of irradiation time, due to the rapid heat dissipation timescales in this regime. When irradiating an L_o domain in a 2:1:1 DOPC/DPPC/Chol GUV for 4 min at 100 mW laser power at the trap no mixing was observed, as this was still below the laser power where a miscibility transition occurred. We measured the area of the L_o domain over time, and indeed this remained constant over the timescale of the experiments (Supplementary Fig. 2).

Discussion

We show that membrane domains can be assembled, mixed, demixed and directly manipulated with spatiotemporal control using optical traps. This approach represents a significant milestone toward assembling vesicles with user-defined lateral organisation of membrane content. This is key for the design of new functional membrane-based microsystems. In addition, just as optical traps have proved instrumental in elucidating various aspects of membrane biophysics, our approach can likewise be used to study the physical and mechanical properties of lipid domains, for example by using multi-trap or holographic trapping systems to probe the energetics of domain splitting and reassembly, and by deforming domains away from spherical geometries.

Methods

Vesicle generation. All lipids were purchased from Avanti Polar Lipids (Alabaster, USA), and unless otherwise specified reagents purchased from Sigma Aldrich (Gillingham, UK). GUVs were formed via electroformation. Lipid solutions were prepared with 1 mol% Rh-PE, was first prepared by dissolving appropriate amounts of lipid in chloroform to yield 1 mg ml^{-1} solution. 40 μl of this solution was then spread evenly on an indium tin oxide (ITO) slide, and as the chloroform evaporated a lipid film was deposited. The slide was placed in a desiccator for a minimum of 30 min to remove residual chloroform. A 5 mm thick polydimethylsiloxane (PDMS) spacer with a central cut-out was sandwiched in between two ITO slides, one of which contained the lipid film, with the conductive sides facing each other. This chamber was held together with clips, and was filled with 0.4 M sucrose solution in DI water. An alternating electric field (1 V, 10 Hz) was applied across the ITO plates using a function generator (Aim-TTi, TG315). After two hours, the electric field was changed to 1 V, 2 Hz for a further hour, and the resulting vesicles collected. Domain trapping experiments were conducted with a DOPC/DPPC/Chol 2:1:1 (mol ratio) mixture. GUV compositions for the laser-induced miscibility experiments are given in the text.

Preparing adhered GUVs. Coverslips were first cleaned thoroughly by sonication in detergent (PCC-52, Thermo Fischer Scientific, Waltham, USA) and water for 15 min, followed by extensive rinsing in DI water, and finally by a 2-min plasma treatment (Harrick Plasma Cleaner; Ithaca, USA) to remove any residues on the glass surface. A thin PDMS spacer was used to create a well to which 45 μL of 0.2 M NaCl in DI was added. 5 μL of GUV suspension was then added, and a coverslip placed on top to seal the chamber. Domains were imaged on a Nikon Eclipse TE2000-E under fluorescence using a mercury-fibre illuminator (Nikon Intensilight C-HGFIE), using a TRITC filter with 10 ms camera exposure.

Laser-induced domain mixing. 5 μL of GUV solution containing 0.4 M sucrose was placed in a well containing 95 μL 0.4 M glucose. The well was sealed with a coverslip and the GUVs imaged in fluorescence mode (10 ms exposure TRITC filter). The laser was focussed at the GUV centre, and the power increased at 20 mW (at trap) increments until domain mixing was observed. GUVs were exposed for a maximum of 2 s at every acquisition event to minimise the effects of photo-oxidation processes. All experiments were performed at a room temperature of 21 °C. The objective transmittance and temperature increases due to the laser was quantified using a two-objective measurement method similar to the one described by Misawa et al.[60] as we have adapted previously (Supplementary Table 1)[15].

Data availability

All relevant data are available from the authors upon reasonable request.

Received: 30 April 2018 Accepted: 16 November 2018
Published online: 29 January 2019

References

1. Ashkin, A. & Dziedzic, J. Optical trapping and manipulation of viruses and bacteria. *Science* **235**, 1517–1520 (1987).
2. Piggee, C. Optical tweezers: not just for physicists anymore. *Anal. Chem.* **81**, 16–19 (2009).
3. Grier, D. G. A revolution in optical manipulation. *Nature* **424**, 810 (2003).
4. Fazal, F. M. & Block, S. M. Optical tweezers study life under tension. *Nat. Photonics* **5**, 318 (2011).
5. Arneborg, N. et al. Interactive optical trapping shows that confinement is a determinant of growth in a mixed yeast culture. *FEMS Microbiol. Lett.* **245**, 155–159 (2005).
6. Oddershede, L. B. Force probing of individual molecules inside the living cell is now a reality. *Nat. Chem. Biol.* **8**, 879 (2012).
7. Sitters, G. et al. Optical pushing: a tool for parallelized biomolecule manipulation. *Biophys. J.* **110**, 44–50 (2016).
8. Lanigan, P. M. P. et al. Spatially selective sampling of single cells using optically trapped fusogenic emulsion droplets: a new single-cell proteomic tool. *J. R. Soc. Interface* **5**, S161–S168 (2008).
9. Cecconi, C., Shank, E. A., Bustamante, C. & Marqusee, S. Direct observation of the three-state folding of a single protein molecule. *Science* **309**, 2057–2060 (2005).
10. Clancy, B. E., Behnke-Parks, W. M., Andreasson, J. O. L., Rosenfeld, S. S. & Block, S. M. A universal pathway for kinesin stepping. *Nat. Struct. Mol. Biol.* **18**, 1020–1027 (2011).
11. Wen, J.-D. et al. Following translation by single ribosomes one codon at a time. *Nature* **452**, 598 (2008).
12. Nussenzveig, H. M. Cell membrane biophysics with optical tweezers. *Eur. Biophys. J.* **45**, 499–514 (2017).
13. Friddin, M. S. et al. Optically assembled droplet interface bilayer (OptiDIB) networks from cell-sized microdroplets. *Soft Matter* **12**, 7731–7734 (2016).
14. Dixit, S. S., Kim, H., Vasilyev, A., Eid, A. & Faris, G. W. Light-driven formation and rupture of droplet bilayers. *Langmuir* **26**, 6193–6200 (2010).
15. Bolognesi, G. et al. Sculpting and fusing biomimetic vesicle networks using optical tweezers. *Nat. Commun.* **9**, 1882 (2018).

16. Rørvig-Lund, A., Bahadori, A., Semsey, S., Bendix, P. M. & Oddershede, L. B. Vesicle fusion triggered by optically heated gold nanoparticles. *Nano. Lett.* **15**, 4183–4188 (2015).
17. Veatch, S. L. & Keller, S. L. Separation of liquid phases in giant vesicles of ternary mixtures of phospholipids and cholesterol. *Biophys. J.* **85**, 3074–3083 (2003).
18. Sezgin, E., Levental, I., Mayor, S. & Eggeling, C. The mystery of membrane organization: composition, regulation and roles of lipid rafts. *Nat. Rev. Mol. Cell Biol.* **18**, 361–374 (2017).
19. Binder, W. H., Barragan, V. & Menger, F. M. Domains and rafts in lipid membranes. *Angew. Chem. Int. Ed. Engl.* **42**, 5802–5827 (2003).
20. Brown, D. A. & London, E. Structure and function of sphingolipid and cholesterol-rich membrane rafts. *J. Biol. Chem.* **275**, 17221–17224 (2000).
21. Smart, E. J. et al. Caveolins, liquid-ordered domains, and signal transduction. *Mol. Cell. Biol.* **19**, 7289–7304 (1999).
22. Anderson, R. G. W. & Jacobson, K. A role for lipid shells in targeting proteins to caveolae, rafts, and other lipid domains. *Science* **296**, 1821–1825 (2002).
23. Mayor, S. & Rao, M. Rafts: scale-dependent, active lipid organization at the cell surface. *Traffic* **5**, 231–240 (2004).
24. Rayermann, S. P., Rayermann, G. E., Cornell, C. E., Merz, A. J. & Keller, S. L. Hallmarks of reversible separation of living, unperturbed cell membranes into two liquid phases. *Biophys. J.* **113**, 2425–2432 (2017).
25. Richter, R. P., Bérat, R. & Brisson, A. R. Formation of solid-supported lipid bilayers: an integrated view. *Langmuir* **22**, 3497–3505 (2006).
26. Dietrich, C. et al. Lipid rafts reconstituted in model membranes. *Biophys. J.* **80**, 1417–1428 (2001).
27. Shao, C., Kendall, E. L. & DeVoe, D. L. Electro-optical BLM chips enabling dynamic imaging of ordered lipid domains. *Lab. Chip.* **12**, 3142–3149 (2012).
28. Bagatolli, L. A. Direct observation of lipid domains in free standing bilayers: from simple to complex lipid mixtures. *Chem. Phys. Lipids* **122**, 137–145 (2003).
29. Karamdad, K. et al. Engineering thermoresponsive phase separated vesicles formed via emulsion phase transfer as a content-release platform. *Chem. Sci.* **9**, 4851–4858 (2018).
30. Danial, J. S. H., Cronin, B., Mallik, C. & Walllace, M. I. On demand modulation of lipid composition in an individual bilayer. *Soft Matter* **13**, 1788–1793 (2017).
31. Trantidou, T., Friddin, M., Salehi-Reyhani, A., Ces, O. & Elani, Y. Droplet microfluidics for the construction of compartmentalised model membranes. *Lab. Chip.* **18**, 2488–2509 (2018).
32. Talbot, E. L., Parolini, L., Kotar, J., Di Michele, L. & Cicuta, P. Thermal-driven domain and cargo transport in lipid membranes. *Proc. Natl. Acad. Sci.* **114**, 846–851 (2017).
33. Talbot, E. L., Kotar, J., Parolini, L., Di Michele, L. & Cicuta, P. Thermophoretic migration of vesicles depends on mean temperature and head group chemistry. *Nat. Commun.* **8**, 15351 (2017).
34. Staykova, M., Lipowsky, R. & Dimova, R. Membrane flow patterns in multicomponent giant vesicles induced by alternating electric fields. *Soft Matter* **4**, 2168–2171 (2008).
35. Honerkamp-Smith, A. R., Woodhouse, F. G., Kantsler, V. & Goldstein, R. E. Membrane viscosity determined from shear-driven flow in giant vesicles. *Phys. Rev. Lett.* **111**, 038103 (2013).
36. Sturzenegger, F., Robinson, T., Hess, D. & Dittrich, P. S. Membranes under shear stress: visualization of non-equilibrium domain patterns and domain fusion in a microfluidic device. *Soft Matter* **12**, 5072–5076 (2016).
37. Wurlitzer, S., Lautz, C., Liley, M., Duschl, C. & Fischer, T. M. Micromanipulation of Langmuir-monolayers with optical tweezers. *J. Phys. Chem. B* **105**, 182–187 (2001).
38. Wurlitzer, S., Steffen, P. & Fischer, T. M. Line tension of Langmuir monolayer phase boundaries determined with optical tweezers. *J. Chem. Phys.* **112**, 5915–5918 (2000).
39. Steffen, P., Heinig, P., Wurlitzer, S., Khattari, Z. & Fischer, T. M. The translational and rotational drag on Langmuir monolayer domains. *J. Chem. Phys.* **115**, 994–997 (2001).
40. Smalyukh, I. I., Kaputa, D. S., Kachynski, A. V., Kuzmin, A. N. & Prasad, P. N. Optical trapping of director structures and defects in liquid crystals using laser tweezers. *Opt. Express* **15**, 4359–4371 (2007).
41. Hamai, C., Cremer, P. S. & Musser, S. M. Single giant vesicle rupture events reveal multiple mechanisms of glass-supported bilayer formation. *Biophys. J.* **92**, 1988–1999 (2007).
42. Wu, H.-L., Chen, P.-Y., Chi, C.-L., Tsao, H.-K. & Sheng, Y.-J. Vesicle deposition on hydrophilic solid surfaces. *Soft Matter* **9**, 1908–1919 (2013).
43. Stottrup, B. L., Veatch, S. L. & Keller, S. L. Nonequilibrium behavior in supported lipid membranes containing cholesterol. *Biophys. J.* **86**, 2942–2950 (2004).
44. Seu, K. J. et al. Effect of surface treatment on diffusion and domain formation in supported lipid bilayers. *Biophys. J.* **92**, 2445–2450 (2007).
45. Lingwood, D. & Simons, K. Lipid rafts as a membrane-organizing principle. *Science* **327**, 46–50 (2009).
46. Watanabe, K. et al. High resolution imaging of patterned model biological membranes by localized surface plasmon microscopy. *Appl. Opt.* **49**, 887–891 (2010).
47. García-Sáez, A. J., Chiantia, S. & Schwille, P. Effect of line tension on the lateral organization of lipid membranes. *J. Biol. Chem.* **282**, 33537–33544 (2007).
48. Rinia, H. A., Snel, M. M., van der Eerden, J. P. & de Kruijff, B. Visualizing detergent resistant domains in model membranes with atomic force microscopy. *FEBS Lett.* **501**, 92–96 (2001).
49. Jensen, M. H., Morris, E. J. & Simonsen, A. C. Domain shapes, coarsening, and random patterns in ternary membranes. *Langmuir* **23**, 8135–8141 (2007).
50. Tlusty, T., Meller, A. & Bar-Ziv, R. Optical gradient forces of strongly localized fields. *Phys. Rev. Lett.* **81**, 1738 (1998).
51. Saleh, B. E., Teich, M. C. & Saleh, B. E. *Fundamentals of photonics*. (Wiley, New York, 1991).
52. Svoboda, K. & Block, S. M. Biological applications of optical forces. *Annu. Rev. Biophys. Biomol. Struct.* **23**, 247–285 (1994).
53. Ramsden, J. Molecular orientation in lipid bilayers. *Philos. Mag. B* **79**, 381–386 (1999).
54. Nielsen, M. M. B. & Simonsen, A. C. Imaging ellipsometry of spin-coated membranes: mapping of multilamellar films, hydrated membranes, and fluid domains. *Langmuir* **29**, 1525–1532 (2013).
55. Stone, H. A. & Ajdari, A. Hydrodynamics of particles embedded in a flat surfactant layer overlying a subphase of finite depth. *J. Fluid. Mech.* **369**, 151–173 (1998).
56. Dent, M. R. et al. Imaging phase separation in model lipid membranes through the use of BODIPY based molecular rotors. *Phys. Chem. Chem. Phys.* **17**, 18393–18402 (2015).
57. Chenlo, F., Moreira, R., Pereira, G. & Ampudia, A. Viscosities of aqueous solutions of sucrose and sodium chloride of interest in osmotic dehydration processes. *J. Food Eng.* **54**, 347–352 (2002).
58. Saffman, P. & Delbrück, M. Brownian motion in biological membranes. *Proc. Natl. Acad. Sci.* **72**, 3111–3113 (1975).
59. Saffman, P. Brownian motion in thin sheets of viscous fluid. *J. Fluid. Mech.* **73**, 593–602 (1976).
60. Misawa, H., Koshioka, M., Sasaki, K., Kitamura, N. & Masuhara, H. Three-dimensional optical trapping and laser ablation of a single polymer latex particle in water. *J. Appl. Phys.* **70**, 3829–3836 (1991).

Acknowledgements

This work was supported by the EPSRC via grant EP/J017566/1 and by EPSRC Fellowship EP/N016998/1 awarded to Y.E.

Author contributions

M.S.F. and Y.E. performed the experiments and G.B. developed the mathematical models and biophysical theory. Y.E. and G.B. analysed the data. A.S.R. and G.B. built the optical trapping setup. M.S.F., G.B., A.S.R., O.C., and Y.E. contributed to designing the experiments, discussions and writing the manuscript. Y.E. supervised the project.

Additional information

Supplementary information accompanies this paper at https://doi.org/10.1038/s42004-018-0101-4.

Competing interests: The authors declare no competing interests.

Reprints and permission information is available online at http://npg.nature.com/reprintsandpermissions/

Publisher's note: Springer Nature remains neutral with regard to jurisdictional claims in published maps and institutional affiliations.